

## SMALL-SCALE VARIABILITY OF RAINFALL IN THE TROPICAL AND SUB-TROPICAL REGIONS

A. K. Varma and G. Liu

Department of Meteorology, Florida State University, Tallahassee, Florida 32306

### 1. INTRODUCTION

Rainfall is a highly variable atmospheric parameter with natural spatial variability varying from few meters to several hundreds of kilometers [Tustison et al. 2003]. Understanding the characteristics of the horizontal variability has many implications to, for example, hydrology and satellite remote sensing. For satellite passive microwave measurements of precipitation, it is important to understand this variability to undertake the corrective measures for so called beam-filling problem.

López [1996] reported that frequency distributions obtained for maximum attained echo area and height form radar observations of tropical disturbances are lognormal. Tustison et al. [2003], discussing the scale dependency of the representativeness error associated with interpolation of precipitation from one scale to another. Varma et al. [2004] demonstrated the use of pixel scale variability of rainfall in tackling the beam-filling problem associated with satellite-borne microwave radiometers.

The main thrust of this paper is to understand the variability of the precipitation at typical passive microwave radiometric pixel scale (~25 – 50 km). The two important attributes of the variability – the fractional rain cover and the probability distribution of the precipitation within the pixel-scale are studied.

A comparative study of the distribution from different radars is carried out, and discussed in terms of their geolocations and precipitation forms.

### 2. DATA

The study uses radar data from 7 different radars as listed in table 1. Five of these radars located at Darwin, Guam, Houston, Kwajalein, and Melbourne are from TRMM validation mission. For validation radars, the convective and stratiform cases are separated and studied separately. Out of 7 radars, 4 existed in tropics and the 3 in sub-tropical regions.

The period of processed data and their spatial resolution is given in table 1.

TABLE-1

Radar	Period	Data resolution
Gunnpt-Darwin	Jan-Feb, 1998	2 km
Guam	Jul-Oct, 1998	2 km
Houston	Aug-Sep, 1999	2 km
Kwajalein	Jan-Dec, 1998	2 km
Melbourne	Jul-Aug, 1999	2 km
Japan	Jul-Mar, 0003	5 km
TOGA-COARE	Nov '91-Feb '92	2 km

### 3. ANALYSIS AND RESULTS

In the present study, we focus upon two characteristics of the sub-pixel scale precipitation: the fractional raining area and the distribution of precipitation within a pixel. For both characteristics, the pixel area of 25x25 km is assumed and results are accordingly generated. For Japan and TOGA radars the results are generated for 50X50 km pixel area also. In the following text of this paper we will refer this area as windows.

The study is carried out by defining a window of the size as mentioned above and moving that window one pixel at a time over the entire radar-covered area in both south-north or west-east directions. This allows generating a large number of window-data samples for further analysis of fractional rain cover and to generate conditional probability distribution function for the sub-window rain for given window averaged rain.

#### 3.1 Fractional Rain Cover

The 25 km window allows about 25 pixels in case of Japan radar and about 144 pixels in case of other radars in a window. This window is moved one radar pixel at a time to create several millions of window-data samples for each radars, for the whole period of the availability of the data of the respective radar. The average rain ( $R_{av}$ ) in each window and fractional rain cover (FRC) are computed. This process is done separately for convective and stratiform rain for PR validation radars. A window is considered convective if more then one-third raining radar pixels in the window are found convective. In Fig.1 (a), we have plotted  $R_{av}$  versus FRC averaged in each 0.5% bin of FRC for window sizes of 25 km x 25 km, and 50 km X 50 km for Japan radars with hollow symbols of circle and diamond, respectively. Fig. 1 (b) shows the similar plots for TOGA radar. In case of both the radars and both the windows, the FRC increases with  $R_{av}$ , and reaches unity at  $R_{av} \sim 1$  to 2 mm h<sup>-1</sup>. An exponential function of the following form is fitted to window size of 25 km X 25 km and also plotted as solid line in the figure:

$$FRC(\%) = 100 [1 - a \exp(-bR_{av})] \quad (1)$$

where FRC is in percentage,  $R_{av}$  is in mm h<sup>-1</sup>, and  $a$  and  $b$  are coefficients. For the Japan-radar data, this function fits with a correlation coefficient ( $r$ ) of 0.98 and root mean square (rms) error of 5.7, with  $a=0.9821$  and  $b=4.117$ . For TOGA-radar, the function and for 25 km x 25 km window this function fits with  $r=0.97$ ,  $rms=7.0177$ ,  $a= 1.0381$  and  $b=0.7571$ .

Figure 3 shows the FRC vs  $R_{av}$  plots separately for convective and stratiform cases for all five PR validation radars.

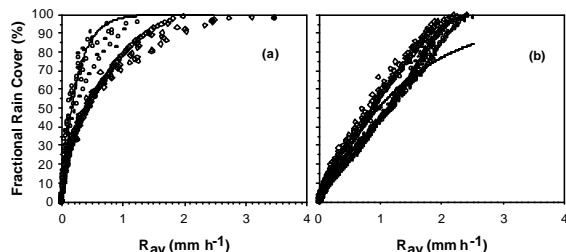


Fig1: Fractional rain cover versus average rain for 25X25 km (circle) and 50X50 km (diamond) window for (a) Japan radar (b) TOGA-radar.

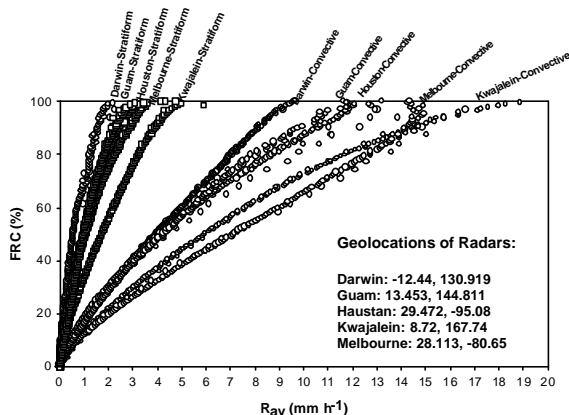


Fig. 2: Fractional rain cover versus average window rain, separately for convective (circle) and stratiform (diamond), for 25X25 km window for 5 radars.

Fig. 1 shows that FRC depends upon the window size. This dependency is prominent in case of Japan radar. Slope of FRC for 25X25 km is steeper compared to 50X50 km window. It is in agreement with the general perception that smaller the size of window, the quicker would it be filled by the rain. This, however, does not appear true for TOGA-radar.

The Fig. 2 shows that the relationship between FRC and  $R_{av}$  is different for convective and stratiform rains. The slope of curves for the stratiform rain is steeper compared to those for convective rain. This is possibly because the stratiform rain is more uniform compared to convective rain. The Fig 2 also reveals that the FRC- $R_{av}$  relationship depends upon the geolocation of the observations.

### 3.1 Probability Distribution Function of Rain

All radar data are analyzed to study the sub-pixel probability distribution of precipitation in 25X25 km window. The average rain rate  $R_{av}$  in each window and the conditional probability distribution function (PDF) of logarithmic radar-pixel rain rate  $[\ln(R)]$  are computed for  $R_{av}$  from 1 -40  $\text{mm h}^{-1}$  with 1  $\text{mm h}^{-1}$  increment. In Fig. 3, the conditional PDF for  $R_{av}$  14-15  $\text{mm h}^{-1}$  for all 7 radars is shown as scatter plot. The conditional PDFs for other  $R_{av}$  bins show similar patterns. The PDF for PR validation radars for

convective and stratiform cases is separately plotted with symbols of circles and boxes, respectively.

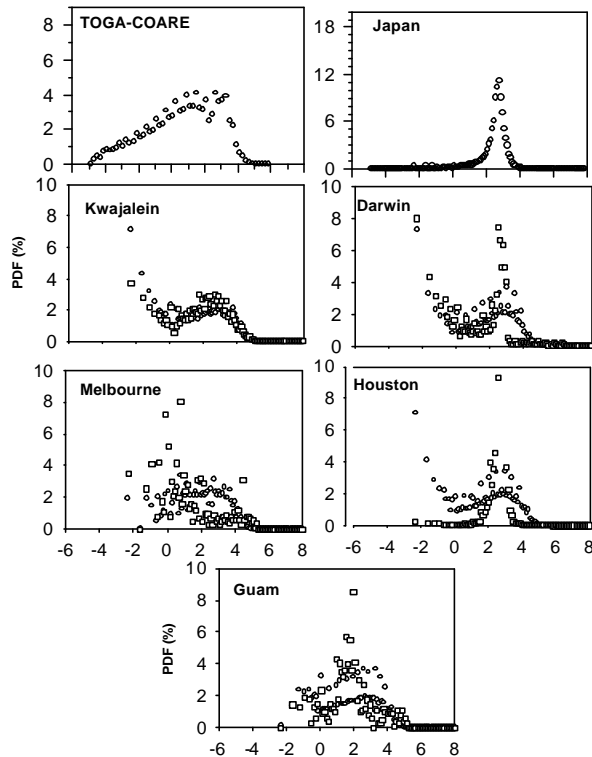


Figure 3: Conditional PDF of logarithmic rain for  $R_{av} = 14-15 \text{ mm h}^{-1}$ . Convective (circle) and stratiform (boxes) cases from PR validation radars are plotted separately.

The PDF of all radars show a Gaussian distribution of logarithmic rain. There, however, variation exists in the form of the Gaussian distribution for different radars for their geolocations and also for rain type.

### 4. CONCLUSION AND DISCUSSIONS

The study demonstrates that FRC Vs  $R_{av}$  depends upon type of rain and also to lesser extent on geolocation of observations. The conditional PDF also shown to vary with geolocation of the observation and the type of the rain (convective or stratiform).

### 5. REFERENCES

- Tustison, B., E. Foufoula-Georgiou, and D. Harris, *J. Geophys. Res.*, **108**, doi:10.1029/2001JD001073, 2003.  
 López, R.E., *Mon. Wea. Rev.*, **104**, 268-283, 1976.  
 Varma, A.K., Guosheng Liu and Yoo-Jeong Noh, Sub-Pixel Scale Variability of Rainfall and Its Application to Mitigate the Beam-Filling Problem, Submitted to *Jour Geophys. Res.*

**Acknowledgments.** This research is supported by NASA under grant NNG04GB04G.